Heat and momentum sources of mean circulation at an altitude of 70 to 100 km

By A. EBEL, *Institute of Geophysics and Meteorology, University of Cologne, FRG*

(Manuscript received April 9; revised version October 3, 1973)

ABSTRACT

Provided that the mean zonal and meridional wind components are known the average vertical velocity component and the momentum and heat sources of the mean meridional circulation can be evaluated applying the steady state equations of the forced mean circulation. Monthly meridional cross sections of pressure, temperature and wind given by Groves (1971, 1969) have been used to determine the mean vertical motion and the rates of momentum and heat changes which are required to maintain the mean circulation as described by the cross sections in the region from 70–100 km altitude. Naturally, the results completely depend on the empirical wind model chosen. A striking feature of this model is the occurrence of mean meridional wind components nearly as large as the zonal components. The strong mean meridional winds, often ascribed to an insufficient amount of observations, implies large vertical velocity components, which would lead to effects contradictory to the actual behaviour of the atmosphere if the wind model were very inaccurate. Yet the calculated results correspond with circulation processes postulated from various phenomena such as for instance, the radio wave absorption of the lower ionosphere and seasonal composition changes in the thermosphere. Therefore it is supposed that large mean meridional velocities as given in Groves' (1969) model on the whole reflect the behaviour of the upper mesosphere and lower thermosphere. The resulting seasonal and spatial variations of the heat and momentum sources lead to the assumption that very effective transport processes exist in the region between 70 and 100 km height and that they are caused by fluctuations (for instance waves of different types) which cannot simply be simulated by an eddy diffusion coefficient.

1. Introduction

In studies of the general circulation in the lower atmosphere it is a well known method to treat the mean meridional circulation as partly forced by small-scale and large-scale eddy transports of momentum and heat. These transports appear as additional sources (and sinks) besides the heat and momentum sources of radiation, friction, and other processes. For investigations of the upper atmosphere it is of great interest to know the influence of eddy transports on the observed average field of motion and temperature. This study is concerned with the atmospheric region from about 70 to 100 km. In this region it is impossible to obtain the characteristics of the large-scale eddy transports in the same direct way as in the lower atmosphere by using e.g. daily weather maps. Hence we have to look for indirect information on momentum and heat sources in the upper atmosphere. The steady state equations of the forced mean meridional circulation as given by Gilman (1964) reveal such information if they are applied to the observed mean temperature and velocity field of the upper mesosphere and lower thermosphere. It is the aim of this study to demonstrate that such an analysis can lead to at least plausible results on the dynamics of that region even if, compared with the lower atmosphere, only a relatively small amount of observations is available. The equations of the mean meridional circulation are given in Section 2. The influence of the different heat and momentum sources is obtained as the sum of the source strengths resulting from a mixture of different processes some of which are absent or inefficient in the lower atmosphere, for instance chemical reactions, tidal and gravity wave transports. It is an obvious but regrettable limitation of the proposed method that the effects of these processes cannot be separated. Nevertheless, it will be informative to see the temporal and spatial variations of the sinks and sources and also the vertical motion (Section 3) and compare them with the seasonal and latitudinal changes of some typical upper atmospheric phenomena (Section 4). The limitations of upper atmospheric data are outlined by Murgatroyd (1969). The crucial point of the intended analysis is the use of average meridional velocities. In contrast to the mean circulation in the lower atmosphere large average N–S wind components are found in the region near the mesopause. The data given by Groves (1969) and discussed in the following sections show mean meridional components nearly as large as the zonal components. This is often thought to be the influence of standing waves on the average values which are derived from observations made at relatively few and not uniformly distributed sites. On the other hand, it cannot be excluded that the vertical motion in the region from 70 to 100 km is more prominent than at lower heights and thus allows strong mean meridional winds. It should be noted that the following analysis based on the preliminary wind model of Groves (1969) can only lead to preliminary results. In the last section some arguments in favour of these results and hence in favour of the gross feature of the wind model used will be discussed.

2. Equations and data

The equations governing the mean circulation have been derived and published by several authors. In this paper the notation of Gilman (1964) is used who refers to Saltzman (1961).

List of symbols

t, φ, λ, p	time, latitude, longitude, pressure as independent variables
u, v	mean zonal and meridional wind (positive W → E and S → N)
ω	dp/dt, time and zonal average
T	mean temperature
a	radius of the earth
f	Coriolis parameter
c_p	specific heat at constant pressure
R	gas constant
M	mean molecular weight of air

The dynamic stability

$$Z = f - \frac{1}{a\cos\varphi}\frac{\partial}{\partial\varphi}(u\cos\varphi) \tag{1}$$

and the static stability

$$\Gamma = \frac{R}{Mc_p}\frac{T}{p} - \frac{\partial T}{\partial p} \tag{2}$$

are defined applying the zonal and time averages u and T. In the following dynamical equations all dependent variables on the left hand side represent averages with respect to time and longitude ($\partial/\partial\lambda = 0$). If steady state conditions ($\partial/\partial t = 0$) and hydrostatic equilibrium are assumed the zonal momentum equation, the thermodynamic equation and the continuity equation are

$$\omega\frac{\partial u}{\partial p} - Zv = G \tag{3}$$

$$\frac{v}{a}\frac{\partial T}{\partial\varphi} - \Gamma\omega = H \tag{4}$$

$$\frac{1}{a\cos\varphi}\frac{\partial}{\partial\varphi}(v\cos\varphi) + \frac{\partial\omega}{\partial p} = 0 \tag{5}$$

G and H represent the sum of all momentum and heat sources expressed as force per unit mass and temperature change, respectively, and include the contributions due to eddy transports, planetary, tidal and gravity wave transports and, possibly, other macroscopic transport processes. The relative importance of these processes is not yet known. Therefore we will generally speak of fluctuation effects or processes. The momentum source ($G > 0$) or sink ($G < 0$) can be written as

$$G = \overline{F} - \frac{1}{a\cos^2\varphi}\frac{\partial}{\partial\varphi}(\overline{u'v'\cos^2\varphi}) - \frac{\partial}{\partial p}(\overline{u'\omega'}). \tag{6}$$

In this equation the bar indicates the zonal and time average, whereas the deviation from the mean (with respect to longitude and time) is indicated by a prime. $\overline{F}$ represents the mean viscous frictional force per unit mass. In contrast to studies on the lower atmosphere frictional effects due to turbulence (small-scale eddies) should not be included in $\overline{F}$. For in

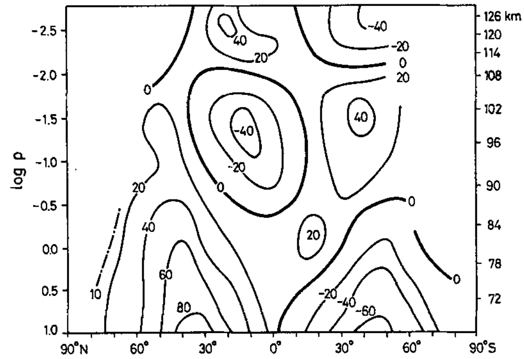

Fig. 1. Quasi-meridional cross section of the mean zonal wind component in m/s for 1 Jan. (northern lat.) and 1 July (southern lat.) after Groves (1969) with $\log p$ as ordinate. p is the pressure in N/m^2. The heights indicated at the right hand side correspond to the equatorial height of the constant pressure levels. Positive winds are towards the east.

most investigations on transport effects above the mesopause the small and large scale eddy and wave transports are jointly treated as "turbulent" diffusion because of the lack of information needed for the separation of the different processes. Thus the general expression "turbulence" is somewhat misleading in the work on the lower thermosphere. Furthermore, it is not clear if the motion in that region is turbulent in a hydrodynamical sense (Layzer & Bedinger, 1969). From composition measurements it can be concluded that viscosity effects are much less important than those of the fluctuations below about 100 km height. Therefore the zonal momentum source G can be regarded as a mere fluctuation parameter in the lower thermosphere.

The heat source in eq. (4) is given by

$$H = \frac{\bar{Q}}{c_p} - \frac{1}{a\cos\varphi}\frac{\partial}{\partial\varphi}(\overline{v'T'}\cos\varphi) - \frac{\partial}{\partial p}(\overline{\omega'T'}) + \frac{R}{M c_p p}\overline{\omega'T'} \qquad (7)$$

where $\bar{Q}$ represents mean diabatic heating rates due to thermal conduction, radiation, chemical reactions, and friction. Similar equations as for the zonal motion can be obtained for the meridional motion and the kinetic energy. In this paper the analysis is restricted to the zonal momentum equation (3) which does not contain the geopotential (because $\partial/\partial\lambda = 0$) and thus enables the determination of a simple fluctuation parameter for the atmospheric motion, whereas the mean energy equation (4) reveals additional information on temperature fluctuations. The evaluation of G and H strongly depends on the quality of the mean meridional circulation data. It is assumed that the data published by Groves (1969) can be accepted for this purpose and that eqs. (3)–(5) can be applied to them (cf. last section).

The wind data are given by Groves for different latitudes, heights, and the first day of each month. Instead of height, pressure is used in this study as the vertical coordinate. The transformation of the original data from the φ, h-system to the φ, p-system is done by means of the pressure tables of Groves (1971). The temperatures are also taken from this publication. Figs. 1 and 2 show the average wind components u and v in January and July. It is assumed that both hemispheres show identical seasonal variations with a phase shift of 6 months (most observations are made in the northern hemisphere and 1 January, south, represents 1 July, north). Groves' original tables contain temperature and pressure values between 0° and 70° latitude up to 110 km height. Values of the mean horizontal wind are given for the region from 60 to 130 km. The latitude range covered by wind data decreases with increasing height. If averages are available up to 70° lat. (wind in the region 60–85 km, T and p up to 110 km) they are extrapolated to 90° lat. assuming that the mean horizontal velocity

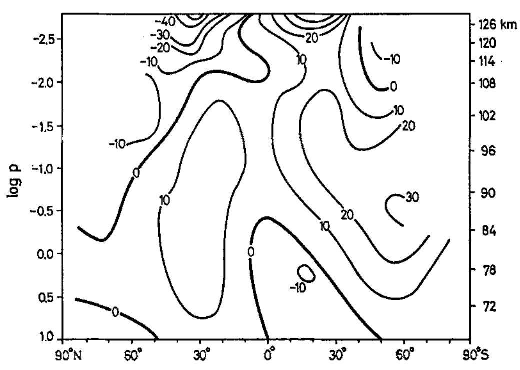

Fig. 2. Quasi-meridional cross section of the mean N–S wind component in m/s, positive towards north. 1 Jan./1 July. Compare the legend of Fig. 1. After Groves (1969).

Table 1. *Evaluation of the wind component w normal to the isobaric surfaces* (1 Jan., 40° latitude)

p = pressure, h = height, Γ = static stability, $\omega = dp/dt$. Negative w means downward motion

p ($\mathrm{Nm^{-2}}$)	h (km)	$1/\Gamma$ ($\mathrm{Km^2N^{-1}}$)	$\dfrac{\partial\omega}{\partial \ln p}$ ($\mathrm{Nm^{-2}\,s^{-1}}$)	ω ($\mathrm{Nm^{-2}\,s^{-1}}$)	w ($\mathrm{cm\ s^{-1}}$)
0.007	112.4	3.7×10^{-5}	1.05×10^{-8}	0.0	0.0
0.011	108.6	7.9×10^{-5}	5.61×10^{-8}	1.0×10^{-8}	−0.7
0.017	105.3	1.7×10^{-4}	1.38×10^{-7}	5.3×10^{-8}	−2.2
0.027	102.2	3.4×10^{-4}	2.36×10^{-7}	1.4×10^{-7}	−3.4
0.042	99.3	6.2×10^{-4}	3.77×10^{-7}	2.8×10^{-7}	−4.1
0.067	96.4	1.0×10^{-3}	4.90×10^{-7}	4.8×10^{-7}	−4.5
0.105	93.6	1.6×10^{-3}	6.89×10^{-7}	7.4×10^{-7}	−4.3
0.165	90.8	2.7×10^{-3}	1.10×10^{-6}	1.1×10^{-6}	−4.1
0.261	88.1	5.4×10^{-3}	1.64×10^{-6}	1.8×10^{-6}	−4.0
0.412	85.4	7.6×10^{-3}	2.44×10^{-6}	2.7×10^{-6}	−3.9
0.649	82.6	1.2×10^{-2}	3.94×10^{-6}	4.1×10^{-6}	−3.8
1.02	79.9	2.0×10^{-2}	6.30×10^{-6}	6.4×10^{-6}	−3.8
1.62	77.0	3.3×10^{-2}	8.36×10^{-6}	9.8×10^{-6}	−3.8
2.55	74.1	5.2×10^{-2}	1.10×10^{-5}	1.4×10^{-5}	−3.5
4.02	71.2	8.3×10^{-2}	1.69×10^{-5}	2.0×10^{-5}	−3.3
6.34	68.1	1.4×10^{-1}	2.32×10^{-5}	3.0×10^{-5}	−3.2

and the mean horizontal temperature and pressure gradients vanish at the pole. Then the temperature and pressure are extrapolated up to heights of 130 km applying the empirical formula of Waldteufel (1970) for the thermospheric vertical temperature profile. The pressure between 110 and 130 km is calculated assuming a linear decrease of the molecular weight of the air from 28.96 at 90 km to 26.05 at 135 km. The extrapolation is carried out to facilitate the numerical treatment of the data. The results described in the following section are only slightly affected beyond 70° lat. and above the pressure level of $\log p \sim -1.7$ (p in $\mathrm{N/m^2}$). Because of the uncertainty of ω above that level the analysis of the velocity field is normally restricted to layers below.

3. Results

The integration of eq. (5) is carried out downward from the uppermost level where $\partial\omega/\partial p$ can be computed and always starts with $\omega_0 = 0$. This procedure evidently leads to large errors of ω near the upper boundary. Yet at lower levels the contribution of the integration constant ω_0 to the computed ω will considerably decrease provided the actual ω_0 is not to large and ω not too small (region of no vertical motion). An estimation of ω_0 can be made by means of the static stability Γ. In eq. (4) the rate of temperature change resulting from the advection term is of the order of 10^{-4} K/s ($v \approx 30$ m/s, $\Delta T \approx 0.5$ K per degree lat.). If a markedly larger value H_x is assumed for the rate of change due to vertical motion the first term of eq. (4) can be dropped and a value ω_x can be determined which will lead to H_x at a height where Γ is given:

$$\omega_x \approx \frac{H_x}{\Gamma} \tag{8}$$

Applying this relation to the upper level where the integration starts the maximum error made by choosing $\omega_0 = 0$ can be determined introducing a reasonably large value of H_x. The following considerations are based on a value $H_x = \pm 10^{-3}$ K/s or ± 86.4 K/day. In Table 1 an example of the integration of $\partial\omega/\partial \ln p = p\,\partial\omega/\partial p$ is given. At the upper level $1/\Gamma = 3.7\times10^{-5}$ N $\mathrm{K^{-1}\,m^{-2}}$ and hence $\omega_x = \pm 3.7\times10^{-8}$ $\mathrm{N\,m^{-2}\,s^{-1}}$. This is the range in which ω_0 can be chosen provided $|\omega\Gamma| < |H_x|$ and thus represents the maximum error of the ω values (fifth column of the table). From the level $p = 0.027$ $\mathrm{N\,m^{-2}}$ ($h = 102.2$ km) downward the error is less than 30% of the computed ω and this percentage

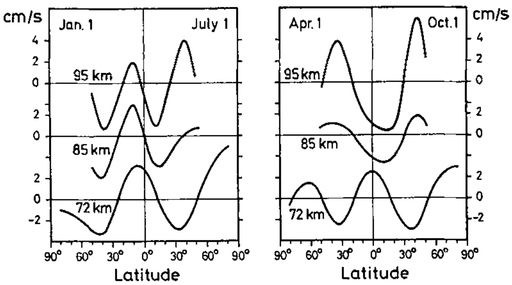

Fig. 3. Latitudinal variation of the mean velocity component w (cm/s) normal to the isobaric surfaces at heights of about 72, 85, and 95 km in the northern hemisphere. Positive values represent upward motion.

value continually decreases as $|\omega|$ increases. Starting the integration at the level 96.4 km ($H_x/\Gamma = \pm 1.0 \times 10^{-6}$ N m^{-2} s^{-1}) the error of ω would be less than 30% from about 90 km altitude downward. Similar conditions as in the case demonstrated in Table 1 are found at all seasons and latitudes with two exceptions: (*a*) At latitudes poleward of 50° the integration has to start at lower levels because of the lack of data above approximately 90 km altitude. This leads to larger values of ω_x ($\approx \pm 10^{-6}$ N m^{-2} s^{-1}). (*b*) In regions where $\omega \approx 0$ large absolute errors have to be taken into account. Fortunately, this only applies to a very small fraction of the analysed data. In some of the following figures dashed lines indicate the regions where all values within the framework of the applied model presumably exceed the error of approximately 30%. Based on the above considerations these regions are determined by a simplified procedure: Below and at 40° latitude the level is determined where $|\omega|$ normally exceeds a value of 5×10^{-7} N m^{-2} s^{-1} progressing from upper to lower levels. At higher latitudes a value of 5×10^{-6} N m^{-2} s^{-1} has been adopted.

The last column of Table 1 contains the velocity component w (cm/s) normal to the isobaric surfaces, computed from ω. Further results for w are shown in Fig. 3 demonstrating the latitudinal variation at three levels near the solstices and equinoxes. Interpreting the values of July and October formally as results from the southern hemisphere one can say that during the equinoxes the zones of upward and downward motion are nearly symmetrically distributed with respect to the equator. Regions with downward motion above the mesopause are found above regions with upward motion below the mesopause and vice versa. Near the solstices the antisymmetrical distribution of zones with downward and upward motion is obvious at the levels above the mesopause. The curve for w at 72 km height seems to be composed of a symmetrical and an antisymmetrical part, the latter showing the well known downward motion in the winter hemisphere and upward motion in the summer hemisphere. It is interesting to note that during the winter, downward motion exists at all heights between about 30° and 50° lat. and upward motion between 5° and 20° lat. More detailed information on the distribution of w with respect to height and latitude can be obtained from the cross-sections for the heat source H (Figs. 5 and 6). The contour lines of H are nearly identical to those of w (negative values in regions of downward motion).

To demonstrate the predominance of the dynamic stability term in eq. (3) the momentum sources are computed in two different ways. Firstly, eq. (3) has been applied introducing ω from eq. (5). Secondly, ω has been replaced by the value which is obtained from eq. (4) when no heat sources are present. The results in Fig. 4 (40° lat., 1 Jan. and 1 July, curves a and b)

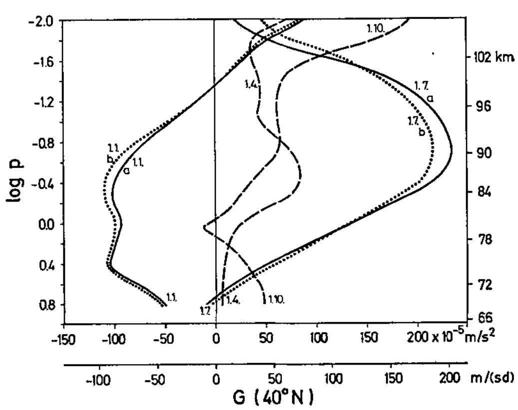

Fig. 4. Vertical profiles of the momentum source G for 1 Jan. (1.1.), 1 April (1.4.), 1 July (1.7.) and 1 Oct. (1.10.) at 40° N. The horizontal scales represent momentum changes per unit mass and per second (upper scale) and per day (lower scale). The height indicated to the right corresponds to the altitude of the constant pressure surfaces at 1 April. Continuous and broken curves: Heat sources present. Dotted curves b: Without heat sources. Pressure in N/m^2.

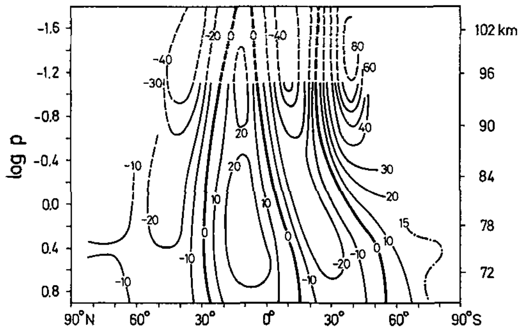

Fig. 5. Quasi-meridional cross section for the source strength H in 10^{-5} K/s (or 0.864 K/d), 1 Jan./1 July, p in N/m². The right vertical scale gives the height of the constant pressure levels at the equator. Dashed lines indicate the regions with errors of the ω integration presumably larger than 30 %.

clearly show that the accuracy of the values for the momentum sources G is more dependent on the accuracy of the mean meridional velocity than on that of the vertical velocity component. The equinoctial profiles of G (1 Apr. and 1 Oct.) are calculated including ω from eq. (5). It is evident from the profiles that the layers from about 70 to 100 km height at 40° lat. act as heat sinks during the winter and change to heat sources during the summer. A reversal takes place somewhere near the equinoxes. The large values of G may now justify the neglect of $\partial u/\partial t$ in eq. (3). A similar argument (large H) holds for $\partial T/\partial t$ as can be seen from the following results.

As already mentioned the heat sources H in the upper atmosphere reflect the changes of the vertical motion with respect to altitude, height, and season. H is very nearly symmet-

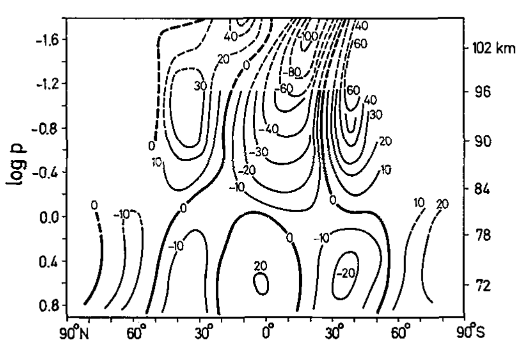

Fig. 6. Distribution of the heat sources H (in 10^{-5} K/s) at 1 April/1 Oct. Compare the text of Fig. 6.

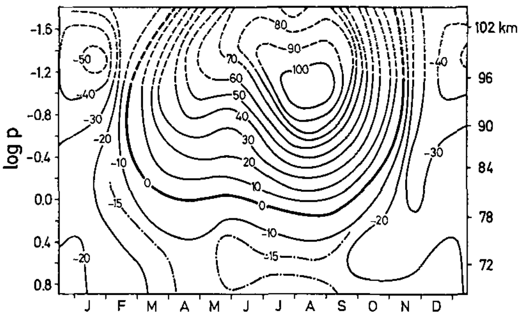

Fig. 7. Seasonal variation of the heat source H (in 10^{-5} K/s) at 40° N. The height scale (right hand side) corresponds to 1 April. Pressure in N/m².

rically distributed in the upper mesosphere and antisymmetrically in the lower thermosphere during the solstices (Fig. 5). The transitional region extends from about 75 to 85 km. The absolute values are somewhat greater in the summer hemisphere. Near the equinoxes (Fig. 6) the distribution of H tends to be symmetrical in the whole region up to about 95 km. Unfortunately, the change in symmetry above 100 km is based on less reliable date, so we must dispense with the discussion of the implications arising from the seasonal asymmetry regarding temporal variations of other atmospheric parameters. The seasonal changes of H are shown in Fig. 7 for 40° N. The 12-month-period is the predominant variation at all levels. Comparing Figs. 5, 6 and 7 one finds that a change of phase of the annual variation occurs between high and low altitudes above about 85 km.

Later on some arguments will be given to the effect that the main contribution to the heat sources probably comes from transport processes due to fluctuations caused by waves or eddies. In the light of such an interpretation the upper mesosphere near 40° lat. is a region from which heat has to be transported throughout the year (negative H due to downward motion below 78 km altitude, Fig. 7). The location to which the heat is transported cannot be identified by the method described in the foregoing section, but is seems reasonable to assume that the main transport is directed to regions with positive H. In the case of horizontal transport such regions are found in the equatorial zone of the upper mesosphere and, with the exception of the winter months, at high latitudes (Figs. 5 and 6). In the vertical direction such regions are found in the lower thermosphere from March to October. If vertical transport takes place during the winter it must penetrate the lower and/or upper boundary of the analysed region because no layers with positive H are present near 40° lat. In particular, the seasonal variation of such vertical transports is of interest for the theory of upper atmosphere dynamics. This will be seen in the next section after discussing some indications which may support the results on mean momentum and heat sources as derived from Groves' wind model.

4. Discussion and concluding remarks

The most convenient parameter for checking the applicability of the empirical meridional circulation model published by Groves (1969) is the vertical velocity component. For we have to see whether our results agree with other observed phenomena and their theoretical—or hypothetical—explanation which is often given in terms of vertical motion. The only information on mean horizontal winds which is not included in the analysed circulation model comes from the observation of noctilucent clouds. One finds an average motion of 40–50 m/s towards SW (Fogle, 1972; Schroeder, 1972) for summer conditions near the mesopause at 50° to 60° N. This agrees fairly well with the corresponding average velocity of Figs. 1 and 2.

Observations of the radio wave absorption in the lower ionosphere have a good spatial resolution and may provide us with more comprehensive arguments for the validity of the results described in the last section. It is now generally accepted that the absorption and especially the winter anomaly of absorption strongly depends on the dynamics of the lower thermosphere, the mesosphere, and maybe the stratosphere (Schwentek, 1968; Labitzke & Schwentek, 1968; Gregory & Manson, 1969; Sechrist, 1972). The winter anomaly is characterised by an enhancement of the absorption at middle and high latitudes during the winter and is confined to the layer above about 85 km (Laštovička, 1972). Regarding the latitude dependence between 30° and the polar region one finds a clear antisymmetry with respect to the equator with increasing absorption values towards the polar region in the winter hemisphere and decreasing values in the summer hemisphere.

Below the mesopause the absorption behaves quite normally with a maximum in the summer and a minimum in the winter caused by the variation of the suns ionizing radiation. Similar differences between the layers above and below the mesopause are found for the change of the vertical motion (Fig. 3). Above 85 km and at latitudes $|\varphi| \geqslant 30°$ downward motion apparently corresponds to the anomalous absorption regime and vice versa. The equatorward boundary of the anomaly appears as the region of reversal from downward to upward motion.

From Fig. 3 a trend to upward motion in the summer hemisphere and downward motion in the winter hemisphere is obvious at all levels. Such a circulation system has been postulated by Kellog (1961) to explain the warm winter mesopause and cold summer mesopause. Vertical motion influences the composition of the thermospheric gas mixture by generating departures from diffusive equilibrium conditions and/or causing seasonal changes of the composition near the so-called turbopause. Therefore circulation systems similar to that derived in Sect. 3 and extending to layers above the analyzed region have often been used for the interpretation of the seasonal anomaly of the ionospheric F-layer (anomalous large electron density in winter at middle and high latitudes, cf. e.g. Yonezawa, 1959) and are now widely adopted as a possible explanation of the thermospheric winter Helium and summer Argon bulge over the polar caps (e.g. Johnson & Gottlieb, 1970).

A most interesting support for the analysis carried out in this paper comes from theoretical considerations of Volland & Mayr (1972) on thermosphere dynamics. They derived predominantly antisymmetric wind cells for solstice conditions and symmetric modes for equinoctial conditions. Comparing their results with the vertical motion shown in Fig. 3 one can interprete the curves for January/July above the mesopause as superposed wind cells, one extending from the summer pole with an upward flow to the winter pole with a downward flow (mode 1) and the other three situated between 40° S and 40° N (presumably mode 5, i.e. five wind cells between the poles). During the equinoxes the symmetric mode 4 (four cells) is the prevailing mode in the lower thermosphere

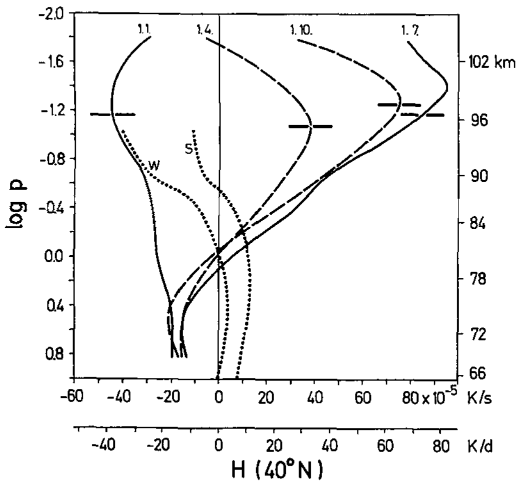

Fig. 8. Vertical profile of the heat source H at 1 Jan. (1.1.), 1 April (1.4.), 1 July (1.7.), and 1 Oct. (1.10.). Latitude 40° N. H in K/s (upper scale) and K/d (lower scale); heights at the right hand side of 1 April. The dotted curves show the radiative temperature change derived by Kuhn (1969, 1971) for winter (W) and summer (S) conditions assuming a CO_2 relaxation time of 2×10^{-6} s (STP).

according to Fig. 3 (w Apr./Oct.). Several discrepancies between the theoretical and empirical results will be found, for instance the position of the wind cells or a slight antisymmetry during the equinoxes. Yet they are of minor importance regarding the principal similarities. At the end of Sect. 3 it was suggested that seasonal variations occur in the seasonal heat transport in the layer between 70 and 100 km altitude. The theory of thermospheric density variations is based on time variations of the energy sources one of which is thought to be the atmosphere below the mesopause. It is therefore interesting to note that the period during the winter when the energy flow from below into the thermosphere is probably best developed at 40° lat., corresponds to the period when the thermospheric density maximum of the annual variation is observed. Similar considerations hold for the semiannual density variation regarding the heat sources in the region from 70–100 km altitude at low latitudes.

Supposing now that the empirical circulation model of Groves (1969) leads to at least qualitatively correct results on the heat and momentum sources we can look for processes which may explain the seasonal and latitudinal variations discribed in Sect. 3. From the work of Kuhn (1969, 1971) it follows immediately that radiative processes, which essentially influence the heat balance of the lower thermosphere, cannot themselves produce the calculated distribution of H in Fig. 5 where regions with sources and sinks are found above 90 km. The calculations of Kuhn only yield negative rates of temperature changes in that region. The disagreement between these rates and the heat source H is demonstrated in Fig. 8, for summer and winter conditions including equinoctial H-profiles for comparison. For instance, positive rates are found by Kuhn below the mesopause whereas H is always negative due to downward motion in this special case. The theoretical values are probably too small above the mesopause (Kuhn, personal communication). But revised model parameters will not remove the apparent discrepancy. Similarly detailed comparisons are not possible for other diabatic processes (e.g. chemical heating). Also, they can probably not explain the variations of H. So it must be concluded that "fluctuation processes" essentially contribute to the heat fluxes. That these processes can by no means be simulated by a simple eddy diffusion coefficient K can easily be proven by means of the momentum source G which implies fluxes against the gradient of momentum and thus leads to negative eddy diffusion coefficients in many cases. Regarding this coefficient K as a small-scale eddy parameter, one may infer that large-scale fluctuations, e.g. atmospheric waves, cause the most effective transports of heat and momentum in the upper mesosphere and lower thermosphere. (For a more detailed discussion cf. Murgatroyd, 1971.) As long as we do not know the actual transport processes indicated by the mean circulation we are far from understanding the atmosphere between the mesopause and so-called turbopause.

Acknowledgements

The author would like to thank G. V. Groves, W. R. Kuhn, and R. J. Murgatroyd for helpful correspondence.

REFERENCES

Fogle, B. 1972. Noctilucent clouds—their characteristics and interpretation. In *Thermospheric circulation* (ed. W. L. Webb), pp. 95–107. MIT Press, Cambridge, Mass. and London.

Gilman, P. A. 1964. On the meridional circulation in the presence of a steady state, symmetric, circumpolar vortex. *Tellus 16*, 160–167.

Gregory, J. B. & Manson, A. H. 1969. Seasonal variations of electron densities below 100 km at mid-latitudes-II. Electron densities and atmospheric circulation. *J. Atmosph. Terr. Phys. 31*, 703–729.

Groves, G. V. 1969. Wind models from 60 to 130 km altitude for different months and latitudes. *J. Brit. Interplan. Soc. 22*, 285–307.

Groves, G. V. 1971. Atmospheric structure and its variations in the region from 25 to 120 km. *AFCRL-71-0410, Environm. Res. Papers 368.*

Johnson, F. S. & Gottlieb, B. 1970. Eddy mixing and circulation at ionospheric levels. *Planet. Space Sci. 18*, 1707–1718.

Kellog, W. W. 1961. Chemical heating above the polar mesopause in winter. *J. Meteor. 18*, 373–381.

Kuhn, W. R. 1969. Radiative transfer in the mesosphere. *Aeronomy Rep. 32, Univ. Illionois, Urbana* (ed. C. F. Sechrist, Jr), pp. 38–47.

Kuhn, W. R. 1971. Radiation processes and the distribution of radiative sources and sinks. *NASA Contract No. NASr-54(03), ORA project 036350.*

Labitzke, K. & Schwentek, H. 1968. Midwinter warmings in the stratosphere and lower mesosphere and the behaviour of ionospheric absorption. *Z. Geophys. 34*, 555–566.

Laštovička, J. 1972. On the winter anomaly of ionospheric absorption. *J. Atmosph. Terr. Phys. 34*, 1233–1239.

Layzer, D. & Bedinger, C. F. 1969. Upper-atmosphere winds and their interpretation-II. Turbulence in the lower E-region. *Planet. Space Sci. 17*, 1891–1911.

Murgatroyd, R. J. 1969. Models of the stratosphere and mesosphere. *Aeronomy Rep. 32, Univ. Illinois, Urbana* (ed. C. F. Sechrist, Jr), pp. 26–36.

Murgatroyd, R. J. 1971. Dynamical modelling of the stratosphere and mesosphere. In *Mesospheric models and related experiments* (ed. G. Fiocco), pp. 104–121. D. Reidel Publ. Co., Dordrecht-Holland.

Saltzman, B. 1961. Perturbation equations for the time-average state of the atmosphere including the effects of transient disturbances. *Geof. pura e appl. 48*, 143–150.

Schroeder, W. 1972. Untersuchungen über leuchtende Nachtwolken. *Zeitschr. Meteorol. 23*, 51–55.

Schwentek, H. 1968. Ähnlichkeiten im jahreszeitlichen Verhalten der Stratosphäre und der D- und E-Schicht der Ionosphäre. *Z. Geophys. 34*, 123–146.

Sechrist, C. F., Jr. 1972. Interactions between the neutral atmosphere and the lower ionosphere. In *Thermospheric circulation* (ed. W. L. Webb), pp. 261–325. MIT Press, Cambridge, Mass. and London.

Volland, H. & Mayr, H. G. 1972. A three dimensional model of thermospheric dynamics-III. Planetary waves. *J. Atmosph. Terr. Phys. 34*, 1797–1816.

Waldteufel, P. 1970. A study of seasonal changes in the lower thermosphere and their implications. *Planet. Space Sci. 18*, 741–748.

Yonezawa, T. 1959. On the seasonal and non-seasonal annual variations and the semi-annual variation in the noon and midnight electron densities of the F2 Layer in middle latitudes, II. *J. Radio Res. Labs. Japan. 6*, 651–668.

ИСТОЧНИКИ ТЕПЛА И ИМПУЛЬСА СРЕДНЕЙ ЦИРКУЛЯЦИИ НА ВЫСОТАХ 70–100 *КМ*

Используя стационарные уравнения вынужденной средней циркуляции, можно оценить среднюю вертикальную компоненту скорости, источники импульса и тепла средней меридиональной циркуляции при условии, что средняя зональная и меридиональная компоненты ветра известны. Использованные средние меридиональные разрезы давления, температуры и ветра по Гровсу (1971, 1969) позволили определить среднее вертикальное движение, а также скорости изменения импульса и тепла, требуемые для поддержания средней циркуляции, представленной разрезами на высотах 70–100 *км*.

Естественно результаты полностью зависят от выбранной эмпирической модели ветра. Удивительной особенностью этой модели является наличие средних меридиональных компонент ветра почти столь же больших, как и зональные компоненты. Сильные средние меридиональные ветры, часто приписываемые недостаточному количеству наблюдений, подразумевают большие вертикальные скорости, что может привести к эффектам, противоречащим обычному поведению атмосферы, если модель ветра очень неточная. Все же результаты вычислений соответствуют циркуляционным процессам, которые подсказываются различными явлениями, такими, например, как поглощение радиоволн в нижней ионосфере и сезонные изменения состава термосферы. Поэтому можно предположить, что большие средние меридиональные скорости в модели Гровса (1969) в целом отражают поведение верхней мезосферы и нижней термосферы. Вытекающие из модели сезонные и пространственные изменения источников тепла и импульса приводят к допущению, что на высотах 70–100 *км* осуществляются очень интенсивные процессы переноса, вызываемые флуктуациями (например, волнами различных типов), которые не могут быть описаны просто коэффициентами турбулентной диффузии.